

# Blood Oxygen Level Measurement with a chest-based Pulse Oximetry Prototype System

Collin Schreiner<sup>1</sup>, Philip Catherwood<sup>1</sup>, John Anderson<sup>2</sup> and James McLaughlin<sup>1</sup>

<sup>1</sup>NIBEC, University of Ulster, Newtownabbey, Northern Ireland

<sup>2</sup>Intelesens Ltd, Belfast, Northern Ireland

## Abstract

*This paper presents a prototyped novel chest-based Pulse Oximetry system, and reports on test results from comparative trials with a commercially available finger-based Pulse Oximetry system using several human subjects. The system was iteratively optimized through adjustment of optical component alignment (angular position, component distance, photosensitive area etc.) and through fine-tuning of LED intensity and receiver sensitivity. This work is significant and timely as it provides compelling evidence that  $SpO_2$  measurements from the chest offer a genuine commercial solution for bedside and ambulatory vital-signs monitoring.*

## 1. Introduction

Presently, non-invasive wireless medical devices for the measurement of blood pressure, body temperature, heart rate (ECG) and respiration are available. The wireless measurement of oxygen saturation (Pulse oximetry) is mostly carried out with finger or ear lobe sensors, and occasionally from the toe or nose. These sensors are usually clipped to a body part or wrapped and gelled around a finger or toe in the case of disposable sensors. The conventional sensors handicap the patient in basic body movements and generate motion artefact, thus creating false alarms for clinicians and nursing staff. Poor blood circulation in the measurement area may also corrupt blood saturation readings. In some life-threatening situations blood circulation is limited to the torso and head [1]. Thus the development of a pulse oximetry sensor located in the upper sternum area (that can also be easily incorporated into existing wireless ECG patches from different manufacturers) is highly desirable.

Initial trials with a reflective pulse oximetry evaluation system have shown that oxygen saturation can be

measured from different locations on the chest. Simultaneous blood saturation measurements on the finger and chest showed a significant delay of  $SpO_2$  results when readings were taken from the finger-based system (figure 1). A drop in blood saturation was detected up to 15 seconds later on the finger-based system. Such reductions in measurement delay could be significant for diagnosis and enable the clinician to introduce treatment more rapidly in the occurrence of an emergency.

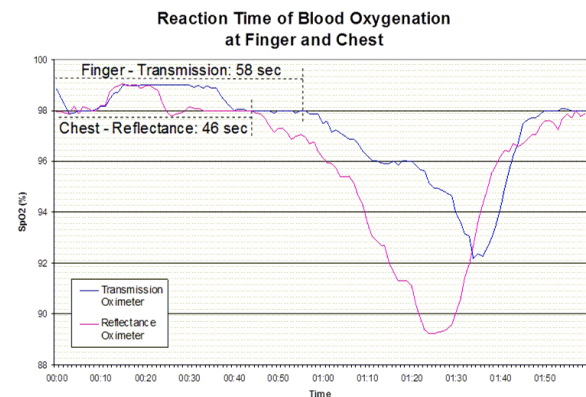


Figure 1.  $SpO_2$  measurements taken simultaneously from a middle finger and chest (upper sternum area) using two Nonin OEM III evaluation kits.

## 1.1. The principle of Pulse Oximetry

The fundamental pulse oximetry 'Ratio of Ratios' concept was invented by [2] and further refined by [3] and [4]. Dual-wavelength illumination of arterial blood results in an absorption contrast that depends upon the proportion of hemoglobin that is chemically combined with oxygen. The colour of blood varies depending on the oxygen content and in particular the hemoglobin molecules reflect more red light when they are oxygenated, whereas, the reflection of infra-red light increases with de-oxygenated hemoglobin molecules.

Precise measurements of the arterial oxygen saturation

can be carried out invasively with co-oximeters. The estimation of  $S_aO_2$ , commonly referred as  $S_pO_2$ , is a function of the measured magnitude at the systolic and diastolic states on the two photoplethysmograms (PPG) (optical recordings of the cardiovascular cycle):

$$\text{Ratio of Ratios} \sim \frac{\ln\left(\frac{\text{Red}_{\text{systole}}}{\text{Red}_{\text{diastole}}}\right)}{\ln\left(\frac{\text{Infrared}_{\text{systole}}}{\text{Infrared}_{\text{diastole}}}\right)}$$

where  $\text{Red}_{\text{systole}}$  and  $\text{Red}_{\text{diastole}}$  are the magnitudes of the red light measured at the systolic and diastolic states respectively, and likewise for  $\text{IR}_{\text{systole}}$  and  $\text{IR}_{\text{diastole}}$ . However, it is essential to note that the 'Ratio of Ratios' (R-curve) has to be empirically calibrated for the specific device in order to produce  $S_pO_2$  in percentage [5].

## 2. The chest-based Prototype System

For the development of a chest-based pulse oximetry system, a single-chip Pulsoximeter design using a MSP430FG439 from Texas Instruments was employed [6]. This system was designed for standard blood saturation measurements when taken on a finger, ear lobe or nose. Such measurements require a transmission pulse oximetry sensor where the LEDs and photodiode are positioned opposite to each other. For the proposed measurements on a chest a reflective sensor was required where the LEDs and photodiode are mounted beside each other. Initially, a simple sensor arrangement was realized by mounting a bi-colour LED (SMT660/910) and a blue enhanced PIN silicon photodiode (PDV-C173SM) onto a PCB board. This enabled the optimal gap size between both components to be experimentally determined during later testing.

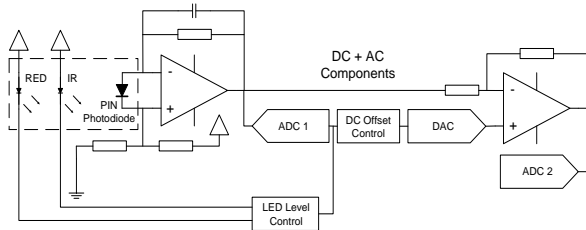


Figure 2. Input front end circuit and LED control of the single-chip Pulsoximeter design using the MSP430.

The main circuit consists of two amplifier stages (figure 2). In the trans-impedance amplifier stage the PIN photodiode is placed across both inputs. In the second stage a DC offset removes a large DC component of the photodiode signal before further amplification. Two readings are taken by a 12-bit ADC module when one LED is switched on. The ADC readings are distinguished by the MCU into two signal pairs (red and infrared). Each

signal pair is processed by the MCU to calculate the current for the individual LED and the required DC offset. The LED current is used to control the illumination of tissue with the aim to obtain the largest possible peak-to-peak amplitude in the amplified photodiode signal. ADC readings of the second amplifier output produce a red and infrared PPG waveform. The baseline of both raw PPG signals varies and sudden signal distortions and baseline shifts are mainly induced by motion artefacts (breathing, movements of the sensor on the chest, etc.). The noise in both PPG signals differs from subject to subject and also depends on the environment (ambient light, electromagnetic interferences (EMI)). The DC residuals and noise in both raw signals are reduced through filtering with a high and low pass digital filter. Processing limitations of the MSP430 made it impossible to apply high order digital filters. Therefore the raw signals were processed by a 2<sup>nd</sup> order high and low pass IIR (Butterworth) filter.

### 2.1. Design of the chest-based Sensor

In the development process three different generations of prototype sensor were built and tested. In the first generation of sensors, the suitability of photodiodes from different manufacturers was investigated. The gap between the sensor components was adjusted by re-positioning the bi-colour LED on double-sided tape. In the second generation of sensors, a new photodiode with a larger photosensitive area ( $7.5\text{mm}^2$ ) and the bi-colour LED were mounted and shielded in a small potting box. The five sensors with different gap sizes between photodiode and bi-colour LED (4-8mm) were held with a test strap on the subject's chest.

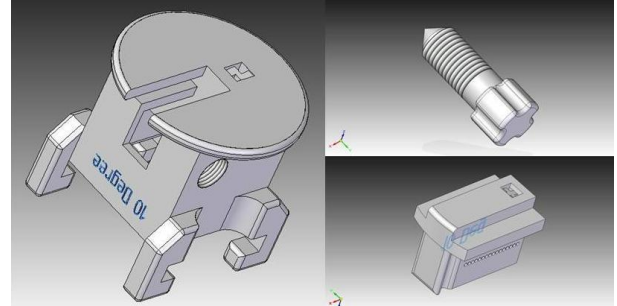


Figure 3. Solid Edge ST images of a housing for a chest-based reflective Pulse Oximetry sensor.

The third generation of sensors were built with housings designed with a 3D CAD application (Solid Edge ST) and printed with a 3D printer (Dimension SST 1200ES). In four sensors the photodiode and LED was rotated by specified angles ( $0^\circ$ ,  $10^\circ$ ,  $20^\circ$ ,  $30^\circ$ ) in respect to the reference plane. An adjusting slider provided gap differences of 6-15mm. In a fifth sensor, the components were rotated by an angle of  $10^\circ$  and elevated above the

reference plane so that the component surface was completely in touch with the skin.

### 3. Results

#### 3.1. Identification of basic $S_pO_2$ parameters and its dependencies

PPG signal detection with photodiodes from different manufacturers was first investigated. As the gap between photodiode and LEDs was gradually increased, the peak-to-peak amplitude of the red and infrared PPG waveforms, LED intensities, DC offsets and the gain of the two amplifier stages were monitored. The photodiodes with a larger sensitive area produced larger peak-to-peak amplitudes. When the gap was increased the LEDs required a higher current. However, a larger gap in most cases produced better signals until the maximum LED current was reached. In general, the infrared PPG waveforms were always better (less noisy, larger peak-to-peak amplitude). Initially, the sensor was identified as the greatest source of noise. For instance, the wiring of the photodiode on the PCB had to be protected with copper foil which in turn was connected to the screen of the supply cable. Noise reduction was also significantly improved through the replacement of the internal MSP430 amplifiers with a low noise high precision trans-impedance amplifier. Additionally, all electronics were mounted into a die-cast aluminium enclosure to protect it against EMI.

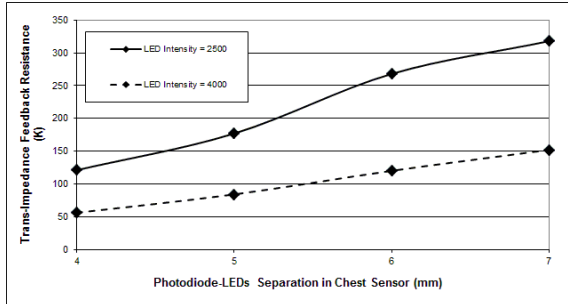


Figure 4. Feedback resistance versus LED intensity.

When first measurements were taken from the chest, recognizable PPG waveforms were only observed when the sensor was placed in the area of a bone (reflection). The much weaker signal (compared to finger measurements) required an increase of gains in both amplifier stages. The best chest signals were accomplished when both LED intensities were set to maximum level and the gain of the trans-impedance amplifier was gradually increased until the signal level at its output was in the upper third area. Higher LED intensities reduced the trans-impedance gain (figure 4).

When the bi-colour LED was driven at its maximum level, the addition of a second bi-colour LED had to be

abandoned due to conflict with wavelength tolerances. Therefore a further improvement was accomplished by increasing the dynamic range of the trans-impedance amplifier through raising the circuit power supply from 3.3V to 5V (figure 5). A larger feedback resistance created larger peak-to-peak amplitudes of the PPG signals, which nearly doubled in size. A higher accuracy in the ADC readings was established by using a 16-Bit ADC to compensate for the larger dynamic range.

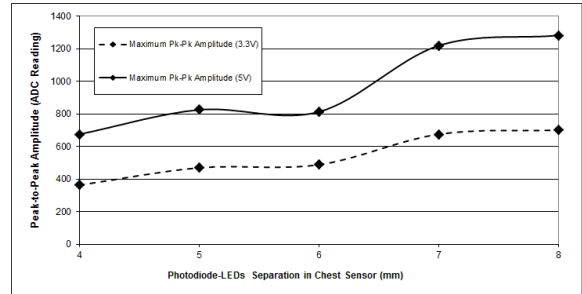


Figure 5. Increased dynamic range for an increased supply voltage (3.3V to 5V).

#### 3.2. Investigation of PPG Signal Detection in respect to Photodiode and LED rotation

Tests with the final 5 sensors (3<sup>rd</sup> generation) have shown that the first sensor (0°) and the fifth sensor (10°, components elevated) detected large peak-to-peak amplitudes, with the latter producing the largest signal. While the second and third sensors (10°, 20°) were able to produce infrared readings only; no acceptable PPG signal was detected when the angular position was 30°. The best red and infrared PPG signals were detected from the fifth sensor with a gap size of 9-10mm. In general the infrared peak-to-peak amplitudes increased further with larger gap size when red readings were not possible.

#### 3.3. Filtering of a chest-based PPG Signal

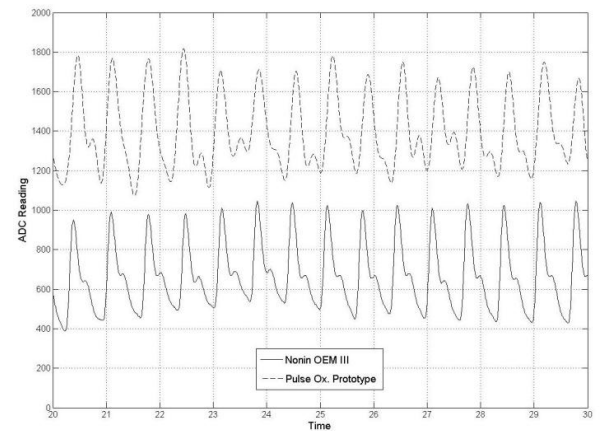


Figure 6. PPG Signals of a Nonin OEM III kit and chest-based Pulse Oximetry Prototype (high order filtering).

In order to compare a chest-based PPG signal of the prototype with a commercial finger-based PPG signal from a Nonin OEM III evaluation kit, simultaneous measurements on one subject were recorded. The data from the prototype system was filtered with a 44<sup>th</sup> order low pass filter (Butterworth, 5Hz cut-off frequency), 20<sup>th</sup> order high pass filter (Butterworth, 0.5Hz cut-off frequency), and finally processed with a moving average filter (20 points) in Matlab. Most of the chest-based waveforms were similar to the waveforms of the Nonin device.

### 3.4. Measurements with a Nonin OEM III and chest-based Pulse Oximetry Prototype

In a final test, data was simultaneously recorded from the middle finger of the left hand (OEM III evaluation kit) and from the chest-based prototype sensor when it was placed in the centre area of the manubrium bone. The subject held the breath as long as possible before returning to breathing normally (SpO<sub>2</sub> test condition). The similarity of the S<sub>p</sub>O<sub>2</sub> (Nonin OEM III evaluation kit) and 'Ratio of Ratios' (Pulse Oximetry prototype) graphs indicate that the chest-based Pulse Oximetry prototype system can be successfully used to measure blood oxygen levels (figure 7 and 8).

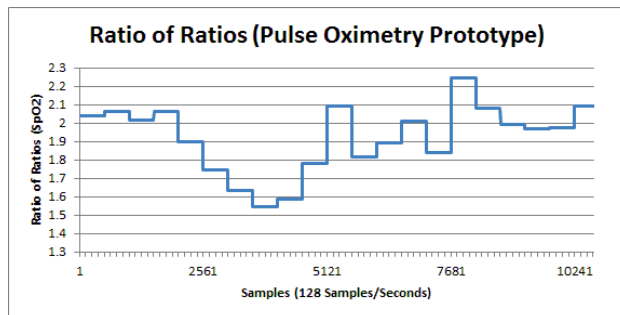


Figure 7. 'Ratio of Ratios' produced by the Pulse Oximetry prototype system (S<sub>p</sub>O<sub>2</sub> test condition).

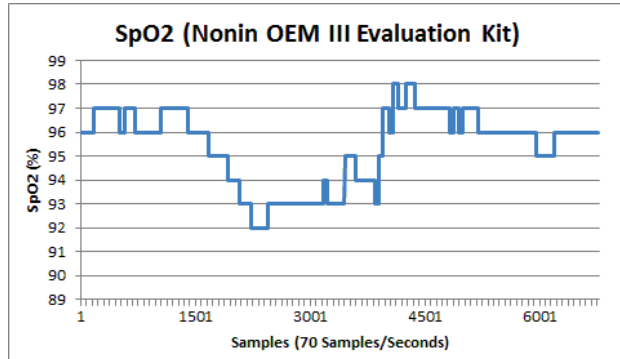


Figure 8. S<sub>p</sub>O<sub>2</sub> values produced by the Nonin OEM III evaluation kit (S<sub>p</sub>O<sub>2</sub> test condition).

## 4. Discussion and conclusions

The development process of a chest-based Pulse Oximetry prototype system and sensors has been presented. After many trials and considerable modification of the electronics and sensor design, many significant parameters for chest-based Pulse Oximetry were identified. S<sub>p</sub>O<sub>2</sub> measurements from a human chest in the upper sternum area requires a high illumination of the tissue (maximum LED light), a large gain (feedback resistance) and boosting of the dynamic range in the trans-impedance amplifier stage (increase of circuit power supply voltage), some angular rotation (i.e. 10°) of photodiode and LEDs in respect to the sensor surface, and elevation so the components completely touch the skin. Additionally, high-order filtering is needed due to PPG waveforms detected with reflective sensors being several times weaker than PPG waveforms detected with a transmission sensor, which results in increased noise and distortion of the signals due to motion artefacts. In conclusion, we have shown SpO<sub>2</sub> can be successfully measured on the upper sternum and the quality and repeatability of measurements are comparable to commercially available finger-based systems. This system offers reduced motion artefact due to positioning and also facilitates integration of SpO<sub>2</sub> measurement into chest-mounted ECG monitoring systems.

## References

- [1] Piantadosi C A "The Biology of Human Survival: Life and Death in Extreme Environments", New York, Oxford University Press, 2003:89-96.
- [2] Aoyagi T, Kishi M, Yamaguchi K, Watanabe S "Improvement of the earpiece oximeter", In: Abstracts of the 13th annual meeting of the Japanese Society for Medical Electronics and Biological Engineering. Osaka, 1974:90-91
- [3] Aoyagi T, Kishi M, Yamaguchi K, Nakajima S, Hirai H, Takase H "New pulse-type ear oximeter", Koyu To Juncan, 1975:23:709-713.
- [4] Yoshida I, Shimada Y, Tanaka K "Spectrophotometric monitoring of arterial oxygen saturation on the fingertip", Med. Biol. Eng. Comput. 1980:18:27-32.
- [5] Webster J G "Design of Pulse Oximeters", New York, Taylor & Francis Group, 1997:40-55.
- [6] Chan V, Underwood S "A Single-Chip Pulsoximeter Design Using the MSP430" (SLAA274), Dallas, Texas Instruments Incorporated, 2005.

Address for correspondence.

Collin Schreiner  
NIBEC, University of Ulster  
Newtownabbey, Co. Antrim  
BT37 0QB  
Northern Ireland  
E-mail: c.schreiner@ulster.ac.uk